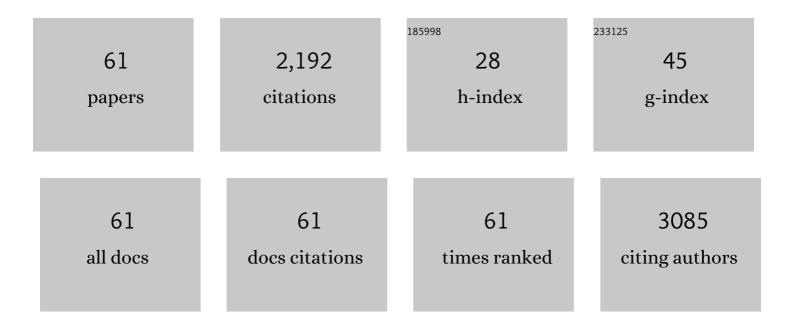
## KwangSup Eom

List of Publications by Year in descending order

Source: https://exaly.com/author-pdf/8261333/publications.pdf Version: 2024-02-01



| #  | Article   | IF  | CITATIONS |
|----|---|-----|-----------|
| 1  | Lignin-Based Materials for Sustainable Rechargeable Batteries. Polymers, 2022, 14, 673.   | 2.0 | 16        |
| 2  | Unraveling the effect of disproportionation of lithium polysulfides on the electrochemical reaction and S utilization in lithium-sulfur battery. Electrochimica Acta, 2022, 412, 140092.  | 2.6 | 5         |
| 3  | Identification of electrode degradation by carbon corrosion in polymer electrolyte membrane fuel cells using the distribution of relaxation time analysis. Electrochimica Acta, 2022, 414, 140219.  | 2.6 | 10        |
| 4  | Enhanced activity and stability of Co-Ni-P-B catalyst for the hydrogen evolution reaction via predeposition of Co-Ni on a Cu substrate. Catalysis Today, 2021, 359, 35-42.  | 2.2 | 14        |
| 5  | Realizing superior energy in a full-cell LIB employing a Li-metal anode via the rational design of a<br>Cu-scaffold host structure with an extremely high porosity. Energy Storage Materials, 2021, 36,<br>326-332.   | 9.5 | 5         |
| 6  | Enhancing the Capacity and Stability of a Tungsten Disulfide Anode in a Lithium-Ion Battery Using Excess Sulfur. ACS Applied Materials & Interfaces, 2021, 13, 20213-20221.   | 4.0 | 8         |
| 7  | Effects of Oversaturated Cathode Humidity Conditions on the Performance Degradation of PEMFCs<br>and Diagnostic Signals of Warburg Impedance under Low Humidity Conditions. Journal of Physical<br>Chemistry C, 2021, 125, 10824-10834.   | 1.5 | 6         |
| 8  | A Comparison Study on the Carbon Corrosion Reaction under Saturated and Low Relative Humidity<br>Conditions via Transmission Line Model-Based Electrochemical Impedance Analysis. Journal of the<br>Electrochemical Society, 2021, 168, 064515.   | 1.3 | 5         |
| 9  | Effects of a nanometrically formed lithiophilic silver@copper current collector on the electrochemical nucleation and growth behaviors of lithium metal anodes. Applied Surface Science, 2021, 554, 149578.   | 3.1 | 11        |
| 10 | Effect of a pre-deposited Ni layer on the hydrogen evolution performance of an electroplated<br>Ni–P/CFP composite catalyst in acidic media. Functional Composites and Structures, 2021, 3, 035001.   | 1.6 | 1         |
| 11 | Understanding an Exceptionally Fast and Stable Li-Ion Charging of Highly Fluorinated Graphene with<br>Fine-Controlled C–F Configuration. ACS Applied Materials & Interfaces, 2021, 13, 53767-53776.   | 4.0 | 9         |
| 12 | Advanced ordered mesoporous carbon with fast Li-ion diffusion for lithium–selenium sulfide<br>batteries in a carbonate-based electrolyte. Carbon, 2020, 170, 236-244.   | 5.4 | 16        |
| 13 | Deconvolution of the dehydration degradation mechanism in polymer electrolyte membrane fuel cells<br>using electrochemical impedance analysis combined with the transmission line model under low<br>humidity. Journal of Power Sources, 2020, 473, 228587.                             | 4.0 | 12        |
| 14 | In Batteria Polyaniline Coating: In Batteria Electrochemical Polymerization to Form a Protective<br>Conducting Layer on Se/C Cathodes for Highâ€Performance Li–Se Batteries (Adv. Funct. Mater. 19/2020).<br>Advanced Functional Materials, 2020, 30, 2070124.                          | 7.8 | 0         |
| 15 | Overcoming the Unfavorable Kinetics of<br>Na <sub>3</sub> V <sub>2</sub> (PO <sub>4</sub> ) <sub>2</sub> F <sub>3</sub> //SnP <i><sub>x</sub></i> Fullâ€Cell Sodiumâ€Ion Batteries for High Specific Energy and Energy Efficiency. Advanced Functional<br>Materials. 2020. 30. 2003086. | 7.8 | 27        |
| 16 | In Batteria Electrochemical Polymerization to Form a Protective Conducting Layer on Se/C Cathodes for Highâ€Performance Li–Se Batteries. Advanced Functional Materials, 2020, 30, 2000028.  | 7.8 | 25        |
| 17 | High-performance boron-doped silicon micron-rod anode fabricated using a mass-producible<br>lithography method for a lithium ion battery. Journal of Power Sources, 2020, 454, 227931.  | 4.0 | 25        |
| 18 | Lithium-selenium sulfide batteries with long cycle life and high energy density via solvent washing<br>treatment. Applied Surface Science, 2020, 512, 145632.   | 3.1 | 9         |

KWANGSUP EOM

| #  | Article   | IF  | CITATIONS |
|----|---|-----|-----------|
| 19 | Amorphous MoSx embedded within edges of modified graphite as fast-charging anode material for rechargeable batteries. Applied Surface Science, 2020, 509, 145352.   | 3.1 | 13        |
| 20 | Enhancing the electrochemical properties of a Si anode by introducing cobalt metal as a conductive buffer for lithium-ion batteries. Journal of Alloys and Compounds, 2020, 827, 154102.  | 2.8 | 27        |
| 21 | Enhancing the electrochemical performances of a tellurium-based cathode for a high-volumetric capacity Li battery via a high-energy ball mill with sulfur edge-functionalized carbon. Journal of Power Sources, 2019, 430, 112-119.   | 4.0 | 22        |
| 22 | Effect of iron content on the hydrogen production kinetics of electroless-deposited Co Ni Fe P alloy catalysts from the hydrolysis of sodium borohydride, and a study of its feasibility in a new hydrolysis using magnesium and calcium borohydrides. International Journal of Hydrogen Energy, 2019, 44, 15228-15238. | 3.8 | 17        |
| 23 | Facile phosphorus-embedding into SnS2 using a high-energy ball mill to improve the surface kinetics of P-SnS2 anodes for a Li-ion battery. Applied Surface Science, 2019, 466, 578-582.   | 3.1 | 20        |
| 24 | Design of Mg-Cu alloys for fast hydrogen production, and its application to PEM fuel cell. Journal of Alloys and Compounds, 2018, 741, 590-596.   | 2.8 | 30        |
| 25 | Corrosion-resistant coating for cathode current collector and wet-seal area of molten carbonate fuel cells. International Journal of Hydrogen Energy, 2018, 43, 11363-11371.  | 3.8 | 6         |
| 26 | In Situ Self-Formed Nanosheet MoS3/Reduced Graphene Oxide Material Showing Superior Performance<br>as a Lithium-Ion Battery Cathode. ACS Nano, 2018, 13, 1490-1498.   | 7.3 | 49        |
| 27 | Selenium-infiltrated mesoporous carbon composite cathode for a high-capacity lithium-chalcogen<br>battery: Effects of carbon structure and dopant on the rate-capability and cyclic stability. Journal of<br>Power Sources, 2018, 408, 111-119.   | 4.0 | 11        |
| 28 | Improving the Stability of an RTâ€NaS Battery via In Situ Electrochemical Formation of Protective SEI on<br>a Sulfur–Carbon Composite Cathode. Advanced Sustainable Systems, 2018, 2, 1800076.  | 2.7 | 14        |
| 29 | Bi-axial grown amorphous MoSx bridged with oxygen on r-GO as a superior stable and efficient nonprecious catalyst for hydrogen evolution. Scientific Reports, 2017, 7, 41190.   | 1.6 | 31        |
| 30 | Submicron silicon encapsulated with graphene and carbon as a scalable anode for lithium-ion batteries. Carbon, 2017, 119, 438-445.  | 5.4 | 53        |
| 31 | Electrospun Nb-doped TiO2 nanofiber support for Pt nanoparticles with high electrocatalytic activity and durability. Scientific Reports, 2017, 7, 44411.  | 1.6 | 53        |
| 32 | A stable lithiated silicon–chalcogen battery via synergetic chemical coupling between silicon and selenium. Nature Communications, 2017, 8, 13888.  | 5.8 | 46        |
| 33 | Fabrication of Mg–Ni–Sn alloys for fast hydrogen generation in seawater. International Journal of<br>Hydrogen Energy, 2017, 42, 7761-7769.  | 3.8 | 49        |
| 34 | Enhancing the Stability of Sulfur Cathodes in Li–S Cells via in Situ Formation of a Solid Electrolyte<br>Layer. ACS Energy Letters, 2016, 1, 373-379.   | 8.8 | 61        |
| 35 | High Temperature Oxidation Behavior of APM and APMT under Dry Air/Steam Condition. MRS Advances, 2016, 1, 2471-2476.  | 0.5 | 2         |
| 36 | Hierarchical networks of redox-active reduced crumpled graphene oxide and functionalized<br>few-walled carbon nanotubes for rapid electrochemical energy storage. Nanoscale, 2016, 8,<br>12330-12338.   | 2.8 | 31        |

KWANGSUP EOM

| #  | Article   | IF  | CITATIONS |
|----|---|-----|-----------|
| 37 | Design of Mg–Ni alloys for fast hydrogen generation from seawater and their application in polymer<br>electrolyte membrane fuel cells. International Journal of Hydrogen Energy, 2016, 41, 5296-5303.   | 3.8 | 77        |
| 38 | Design of an Advanced Membrane Electrode Assembly Employing a Double-Layered Cathode for a PEM<br>Fuel Cell. ACS Applied Materials & Interfaces, 2015, 7, 27581-27585.  | 4.0 | 30        |
| 39 | Improved stability of nano-Sn electrode with high-quality nano-SEI formation for lithium ion battery.<br>Nano Energy, 2015, 12, 314-321.  | 8.2 | 108       |
| 40 | Cobalt-carbon nanofibers as an efficient support-free catalyst for oxygen reduction reaction with a systematic study of active site formation. Journal of Materials Chemistry A, 2015, 3, 14284-14290.  | 5.2 | 77        |
| 41 | A Study on the localized corrosion and repassivation kinetics of Fe-20Cr- x Ni ( x = 0–20 wt%) stainless steels via electrochemical analysis. Corrosion Science, 2015, 100, 158-168.  | 3.0 | 25        |
| 42 | Stabilization of selenium cathodes via in situ formation of protective solid electrolyte layer. Journal of Materials Chemistry A, 2014, 2, 18898-18905.   | 5.2 | 32        |
| 43 | The design of a Li-ion full cell battery using a nano silicon and nano multi-layer graphene composite<br>anode. Journal of Power Sources, 2014, 249, 118-124.   | 4.0 | 110       |
| 44 | Effects of anode flooding on the performance degradation of polymer electrolyte membrane fuel cells. Journal of Power Sources, 2014, 266, 332-340.  | 4.0 | 84        |
| 45 | The effect of fluoroethylene carbonate additive content on the formation of the solid-electrolyte<br>interphase and capacity fade of Li-ion full-cell employing nano Si–graphene composite anodes. Journal<br>of Power Sources, 2014, 257, 163-169.   | 4.0 | 118       |
| 46 | Observation of passive films on Fe–20Cr–xNi (x=0, 10, 20wt.%) alloys using TEM and Cs-corrected<br>STEM–EELS. Corrosion Science, 2014, 79, 34-40.   | 3.0 | 55        |
| 47 | Effects of Dissolved Transition Metals on the Electrochemical Performance and SEI Growth in Lithium-Ion Batteries. Journal of the Electrochemical Society, 2014, 161, A1915-A1921.  | 1.3 | 153       |
| 48 | Optimization of GDLs for high-performance PEMFC employing stainless steel bipolar plates.<br>International Journal of Hydrogen Energy, 2013, 38, 6249-6260.   | 3.8 | 11        |
| 49 | Effects of heat treatment time on electrochemical properties and electrode structure of polytetrafluoroethylene-bonded membrane electrode assemblies for polybenzimidazole-based high-temperature proton exchange membrane fuel cells. International Journal of Hydrogen Energy, 2013. 38, 12335-12342. | 3.8 | 12        |
| 50 | Thermochemical production of sodium borohydride from sodium metaborate in a scaled-up reactor.<br>International Journal of Hydrogen Energy, 2013, 38, 2804-2809.  | 3.8 | 29        |
| 51 | On-board hydrogen production by hydrolysis from designed Al–Cu alloys and the application of this technology to polymer electrolyte membrane fuel cells. Journal of Power Sources, 2012, 217, 345-350.  | 4.0 | 32        |
| 52 | Degradation behavior of a polymer electrolyte membrane fuel cell employing metallic bipolar plates under reverse current condition. Electrochimica Acta, 2012, 78, 324-330.   | 2.6 | 28        |
| 53 | Effects of Pt loading in the anode on the durability of a membrane–electrode assembly for polymer<br>electrolyte membrane fuel cells during startup/shutdown cycling. International Journal of Hydrogen<br>Energy, 2012, 37, 18455-18462.   | 3.8 | 35        |
| 54 | Effects of residual oxygen partial pressure on the degradation of polymer electrolyte membrane fuel cells under reverse current conditions. Journal of Power Sources, 2012, 198, 42-50.   | 4.0 | 27        |

KWANGSUP EOM

| #  | Article   | IF  | CITATIONS |
|----|---|-----|-----------|
| 55 | Design of Al–Fe alloys for fast on-board hydrogen production from hydrolysis. Journal of Materials<br>Chemistry, 2011, 21, 13047.   | 6.7 | 34        |
| 56 | Design of ternary Al–Sn–Fe alloy for fast on-board hydrogen production, and its application to PEM<br>fuel cell. International Journal of Hydrogen Energy, 2011, 36, 11825-11831.   | 3.8 | 42        |
| 57 | Feasibility of on-board hydrogen production from hydrolysis of Al–Fe alloy for PEMFCs.<br>International Journal of Hydrogen Energy, 2011, 36, 12338-12342.  | 3.8 | 38        |
| 58 | Characterization of hydrogen generation for fuel cells via borane hydrolysis using an<br>electroless-deposited Co–P/Ni foam catalyst. Journal of Power Sources, 2010, 195, 2830-2834.   | 4.0 | 52        |
| 59 | Hydrogen generation from hydrolysis of NH3BH3 by an electroplated Co–P catalyst. International<br>Journal of Hydrogen Energy, 2010, 35, 181-186.  | 3.8 | 74        |
| 60 | Effects of deposition time on the H2 generation kinetics of electroless-deposited<br>cobalt–phosphorous catalysts from NaBH4 hydrolysis, and its cyclic durability. International Journal<br>of Hydrogen Energy, 2010, 35, 5220-5226. | 3.8 | 45        |
| 61 | Effects of electroless deposition conditions on microstructures of cobalt–phosphorous catalysts<br>and their hydrogen generation properties in alkaline sodium borohydride solution. Journal of Power<br>Sources, 2008, 180, 484-490. | 4.0 | 125       |